

Fragmentation of star-forming clouds enriched with the first dust

Raffaella Schneider^{1,2}, Kazuyuki Omukai³, Akio K. Inoue⁴ & Andrea Ferrara⁵

¹*Centro Enrico Fermi, Via Panisperna 89/A, 00189 Roma, Italy*

²*INAF/Osservatorio Astrofisico di Arcetri, Largo Enrico Fermi 5, 50125 Firenze, Italy*

³*Division of Theoretical Astronomy, National Astronomical Observatory, Mitaka, Tokyo 181-8588, Japan*

⁴*College of General Education, Osaka Sangyo University, 3-1-1 Nakagaito, Daito, Osaka 574-8530, Japan*

⁵*SISSA/International School for Advanced Studies, Via Beirut 4, 34100 Trieste, Italy*

ABSTRACT

The thermal and fragmentation properties of star-forming clouds have important consequences on the corresponding characteristic stellar mass. The initial composition of the gas within these clouds is a record of the nucleosynthetic products of previous stellar generations. In this paper we present a model for the evolution of star-forming clouds enriched by metals and dust from the first supernovae, resulting from the explosions of metal-free progenitors with masses in the range 12 - 30 M_{\odot} and 140 - 260 M_{\odot} . Using a self-consistent approach, we show that: (i) metals depleted onto dust grains play a fundamental role, enabling fragmentation to solar or sub-solar mass scales already at metallicities $Z_{\text{cr}} = 10^{-6}Z_{\odot}$; (ii) even at metallicities as high as $10^{-2}Z_{\odot}$, metals diffused in the gas-phase lead to fragment mass scales which are $\gtrsim 100M_{\odot}$; (iii) C atoms are strongly depleted onto amorphous carbon grains and CO molecules so that CII plays a minor role in gas cooling, leaving OI as the main gas-phase cooling agent in low-metallicity clouds. These conclusions hold independently of the assumed supernova progenitors and suggest that the onset of low-mass star formation is conditioned to the presence of dust in the parent clouds.

Key words: stars: formation, population III, supernovae: general - cosmology: theory - galaxies: evolution, stellar content - ISM: abundances, dust

1 INTRODUCTION

Supernovae represent the first cosmic polluters. On timescales shorter than 50 Myr, these stellar explosions seed the cosmic gas with the first metals. Theoretical models suggest that a significant fraction of these heavy elements could be in the form of dust grains (Kozasa, Hasegawa & Nomoto 1989; Todini & Ferrara 2001; Nozawa et al. 2003; Schneider, Ferrara & Salvaterra 2004). Indeed, following the explosion, conditions are met in the expanding SN ejecta for the condensation of gas-phase metals in grains of different size and species. In particular, the fraction of metals depleted onto dust, $f_{\text{dep}} = M_{\text{dust}}/M_{\text{met}}$, varies between 0.3 and 0.7 for pair-instability supernovae (PISN) with progenitor masses in the range 140–260 M_{\odot} (Schneider et al. 2004), and between 0.24 and 1 for Type-II supernovae (SNII) with 12 – 30 M_{\odot} progenitors (Todini & Ferrara 2001).

Efficient dust production on short timescales in supernova ejecta provides a straightforward interpretation of the large dust masses ($M_{\text{dust}} \sim 10^9 M_{\odot}$) inferred from mm and submm observations of quasars (QSOs) with redshifts $5.7 < z < 6.42$, (Bertoldi et al. 2003; Priddey et al. 2003).

Dust condensation in the atmospheres of AGB stars requires timescales of 1 - 2 Gyr (Morgan & Edmunds 2003), too long to account for the presence of large dust masses at redshifts $z > 5$, when the age of the Universe is < 1.2 Gyr. Further support to a SN origin for dust at high redshift has recently come from near-IR observations of a $z = 6.22$ QSO (Maiolino et al. 2004). The extinction properties of the observed spectrum cannot be reproduced assuming a Small Magellanic Cloud dust extinction curve (which generally applies to $z < 5$ systems) and can, instead, be interpreted with models for dust produced in SNII ejecta. Still, direct IR observations of SN remnants (Cassiopea A, Crab, Kepler) have detected only thermal emission from a hot dust component (temperatures 50 – 80 K) with associated dust masses of only 0.003 – 0.07 M_{\odot} (Hines et al. 2004; Green et al. 2004). A larger dust component could be at lower temperatures (< 30 K), and thus not visible at IR wavelengths. Submm observations of some of these systems have, so far, yielded only upper limits, with estimated masses $< 0.2 - 1.5M_{\odot}$ (Morgan et al. 2003; Krause et al. 2004; Wilson & Batrla 2005).

Early metal enrichment of the cosmic gas has important

arXiv:astro-ph/0603766v1 28 Mar 2006

implications for the formation of the first low-mass and long-lived stars. In the last few years, results of sophisticated numerical simulations (Abel, Brian & Norman 2002; Bromm, Coppi & Larson 2002) and semi-analytical models (Omukai & Nishi 1998; Omukai 2000; Nakamura & Umemura 2002) have shown that, due to the primordial composition of the gas, the first stars were predominantly very massive, with masses of $100 - 1000 M_{\odot}$. The presence of metals favors cooling and fragmentation of prestellar-gas clouds, enabling the formation of solar and sub-solar mass stars when the gas initial metallicity reaches a critical value Z_{cr} . Despite its importance, theoretical studies have only constrained this fundamental parameter to within a few orders of magnitudes, $10^{-6} Z_{\odot} \leq Z_{\text{cr}} \leq 5 \times 10^{-3} Z_{\odot}$, with the lowest limit implied by models which include the effect of dust cooling (Schneider, Ferrara, Natarajan & Omukai 2002; Schneider et al. 2003; Omukai, Tsuribe, Schneider & Ferrara 2005) and the highest limit suggested by studies where metal line cooling is considered to be the main driver of the transition (Bromm, Ferrara, Coppi & Larson 1999).

All these theoretical studies relies on the assumption that the relative metal abundances and dust grains properties which characterize the initial composition of pre-stellar gas clouds are the same as those observed in the local interstellar medium, simply rescaled to lower values of metallicity. However, the composition of the cosmic gas enriched by nucleosynthetic products of the first stellar generation through supernova explosions is likely to be different. To overcome this basic limitation, Bromm & Loeb (2003) have derived individual critical abundances of C and O but have limited their analysis to CII and OI fine-structure line cooling during the relatively low-density evolution of collapsing pre-stellar clouds.

In this paper, we follow a different approach and study the detailed thermal and fragmentation history of collapsing clouds enriched by the first supernova explosions. We use the model developed by Omukai (2000), and recently improved in Omukai et al. (2005) to carry out the first self-consistent study which explicitly accounts for the relative metal abundances and dust properties predicted by supernova models. We follow the fate of collapsing clouds enriched by these nucleosynthetic products to investigate whether preferred mass scales can be identified, and eventually linked to characteristic masses of second generation stars.

The initial composition of collapsing gas clouds must be inferred by results of stellar and supernova models of metal-free stars. This relies on specific assumptions on the initial mass function (IMF) of Population III stars. Unfortunately, both the mass range and the shape of the IMF are still hampered from our limited understanding of the accretion physics and protostellar feedback effects (Omukai & Palla 2003; Bromm & Loeb 2004; Tan & McKee 2004; see also Bromm & Larson 2004 for a thorough review). Given these uncertainties, we consider Population III stars forming both in the SNII and PISN progenitor mass ranges, taking $22 M_{\odot}$ and $195 M_{\odot}$ stars as representative cases for the two classes.

The paper is organized as follows: in section 2 we describe the characteristics of the model, with particular attention on those aspects which have been specifically introduced to account for the properties of supernova dust grains. In section 3 we present the results of the analysis, and in sec-

tion 4 we summarize the main conclusions and discuss their implications.

2 THE MODEL

The thermal and chemical evolution of star forming gas clouds is studied using the model developed by Omukai (2000) and recently improved in Omukai et al. (2005). The collapsing gas clouds are described by a one-zone approach where all physical quantities are evaluated at the center as a function of the central density of hydrogen nuclei, n_{H} . The temperature evolution is computed by solving the energy equation

$$\frac{de}{dt} = -p \frac{d}{dt} \frac{1}{\rho} - \Lambda_{\text{net}} \quad (1)$$

where the pressure, p , and the specific thermal energy, e , are given by,

$$p = \frac{\rho k T}{\mu m_{\text{H}}} \quad (2)$$

$$e = \frac{1}{\gamma - 1} \frac{k T}{\mu m_{\text{H}}} \quad (3)$$

and ρ is the central density, T is the temperature, γ is the adiabatic exponent, μ is the mean molecular weight and m_{H} is the mass of hydrogen nuclei. The terms on the right-hand side of the energy equation are the compressional heating rate,

$$\frac{d\rho}{dt} = \frac{\rho}{t_{\text{ff}}} \quad \text{with} \quad t_{\text{ff}} = \sqrt{\frac{3\pi}{32G\rho}}, \quad (4)$$

and the net cooling rate, Λ_{net} , which consists of three components,

$$\Lambda_{\text{net}} = \Lambda_{\text{line}} + \Lambda_{\text{cont}} + \Lambda_{\text{chem}}. \quad (5)$$

The first component, Λ_{line} , represents the cooling rate due to the emission of line radiation, which includes molecular line emission of H_2 , HD, OH and H_2O , and atomic fine-structure line emission of CI, CII and OI. Following Omukai et al. (2005), H_2 collisional transition rates and HD parameters are taken from Galli & Palla (1998). The second component, Λ_{cont} , represents the cooling rate due to the emission of continuum radiation, which includes thermal emission by dust grains and H_2 collision-induced emission. The last term, Λ_{chem} , indicates the cooling/heating rate due to chemical reactions. When the gas cloud is optically thick to a specific cooling radiation, the cooling rate is correspondingly reduced by multiplying by the photon escape probability. Unless otherwise stated, the treatment of these processes are the same as in Omukai (2000), to which we refer the interested reader for further details.

In the present analysis, we relax the assumptions that gas-phase elemental abundances and dust grain properties are the same as those observed in local interstellar clouds. Instead, we compute the relative abundances of gas-phase metals and dust grains applying the model of Todini & Ferrara (2001) for metal-free Type-II supernovae (SNII) and of Schneider, Ferrara & Salvaterra (2003) for pair-instability supernovae (PISN). The properties of dust (relative dust compounds and grain size distributions) affect two processes which contribute to the thermal evolution of gas clouds: (i)

the cooling rate due to dust thermal emission and (ii) the H_2 formation rate on dust grains. The description of these processes has been modified with respect to the treatment in Omukai (2000) and Omukai et al. (2005) to properly take into account the properties of dust grains produced in the first supernova explosions.

2.1 Dust cooling

The contribution of dust grains to gas cooling is determined by the balance between dust thermal emission and heating due to collisions with gas particles,

$$4\sigma T_{\text{gr}}^4 \kappa_{\text{P}} \beta_{\text{esc}} \rho_{\text{gr}} = H_{\text{gr}} \quad (6)$$

where σ is the Stefan-Boltzmann constant, T_{gr} is the dust temperature, κ_{P} is the Planck mean opacity of dust grains per unit dust mass, β_{esc} is the photon escape probability, and the dust mass density ρ_{gr} can be expressed as $\rho \mathcal{D}$, with \mathcal{D} indicating the dust-to-gas ratio. Following Omukai (2000) the photon escape probability can be written as,

$$\beta_{\text{esc}} = \min(1, \tau^{-2}) \quad \text{with} \quad \tau = \kappa_{\text{P}} \rho \lambda J, \quad (7)$$

where the optical depth is estimated across one local Jeans length (roughly the size of the central core region in the Penston-Larson similarity solution). The Planck mean opacity per unit dust mass is,

$$\kappa_{\text{P}} = \frac{\pi}{\sigma T_{\text{gr}}^4} \int_0^{\infty} B_{\nu}(T_{\text{gr}}) \kappa(\nu) d\nu \quad (8)$$

where $\kappa(\nu)$ is the absorption coefficient for the frequency ν per unit dust mass and $B_{\nu}(T_{\text{gr}})$ is the Planck brightness.

The right-hand side of the eq. (6) is the collisional heating (cooling) rate per unit volume ($\text{erg s}^{-1} \text{cm}^{-3}$) of dust (gas) particles and can be written as (Hollenbach & McKee 1979),

$$H_{\text{gr}} = \frac{n_{\text{gr}}(2kT - 2kT_{\text{gr}})}{t_{\text{coll}}} \quad (9)$$

where $t_{\text{coll}}^{-1} = n_{\text{H}} \sigma_{\text{gr}} \bar{v}_{\text{H}} f$ is the average time between two successive collisions, n_{gr} and σ_{gr} are the grain number density and cross section, \bar{v}_{H} is the average speed of hydrogen nuclei and $f = \bar{v}/n_{\text{H}}\bar{v}_{\text{H}}$ measures the contribution of other species. We assume that the gas is fully molecular and follows a Maxwellian distribution so that,

$$\bar{v}_{\text{H}} = \left(\frac{8kT}{\pi m_{\text{H}}} \right)^{1/2}, \quad (10)$$

and $f = 0.3536 + 0.5 y_{\text{He}}$, where $y_{\text{He}} = n_{\text{He}}/n_{\text{H}} = 0.083$ (which corresponds to a He mass fraction of $Y=0.25$) and we have neglected the contribution of heavy elements. These are good approximations in the density range where collisional dust heating is relevant ($n_{\text{H}} > 10^{12-13} \text{cm}^{-3}$) and for the gas metallicities that we are interested to ($Z = Z_{\text{cr}}$).

If we further write,

$$n_{\text{gr}} \sigma_{\text{gr}} = n_{\text{H}} m_{\text{H}} (1 + 4y_{\text{He}}) S \mathcal{D} \quad (11)$$

in eq. (9), where S is the total grain cross section per unit mass of dust, eq. (6) appears to be independent of the dust-to-gas ratio and to depend on the thermal states of gas and dust and on grain specific properties (cross section and Planck mean opacity).

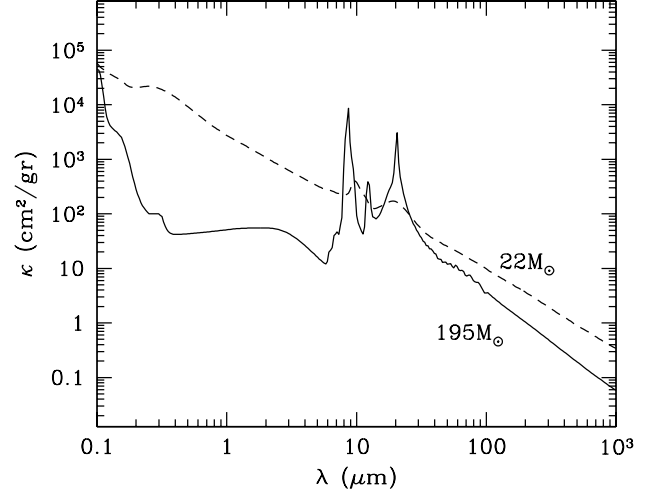


Figure 1. Absorption coefficients per unit dust mass assuming the properties (size distributions and relative masses of different grain species) of dust grains predicted to form in the ejecta of a 195 M_{\odot} PISN (solid lines) and of a 22 M_{\odot} SN (dashed lines).

Given the grain size distribution functions per unit dust mass ($\text{cm}^{-1} \text{gr}^{-1}$), $n_{\text{gr},i}(a) = dn_{\text{gr},i}(a)/da$, and the mass fractional abundance, f_i , of each grain type i predicted by the SN-dust formation models, the total grain cross section per unit dust mass (cm^2/gr) is,

$$S = \sum_i f_i S_i \quad \text{with} \quad S_i = \int_0^{\infty} n_{\text{gr},i}(a) \pi a^2 da. \quad (12)$$

Similarly, the total absorption coefficient per unit dust mass (cm^2/gr) is,

$$\kappa(\nu) = \sum_i f_i \kappa_{\nu,i} \quad \text{with} \quad \kappa_{\nu,i} = \int_0^{\infty} Q_{\nu}^i(a) n_{\text{gr},i}(a) \pi a^2 da, \quad (13)$$

where Q_{ν}^i are the absorption (or extinction) cross section normalized to the geometrical cross-sections. For each dust species, the Q parameters for any frequency and radius have been computed using the standard Mie theory for spherical grains with grain optical constants collected from published data (see Table 1 for details). In Fig. 1 we show the total absorption coefficients per unit dust mass assuming the properties of dust grains formed in the ejecta of a 195 M_{\odot} PISN (see Figs. 4 and 5 in Schneider, Ferrara & Salvaterra 2004) and of a $Z=0$, 22 M_{\odot} SN (see Figs. 5 and 6 in Tordini & Ferrara 2001). For the PISN model, the absorption coefficient is dominated by SiO_2 grains in the 6 μm - 200 μm range, whereas above 200 μm amorphous carbon (AC) grains give a comparable contribution. Shortward of 6 μm , AC grains largely dominate down to $\sim 0.2 \mu\text{m}$, below which Mg_2SiO_4 grains produce the steepening of the curve. For the SNII model, the absorption coefficient is largely dominated by AC grains except for the 0.8 μm - 30 μm range, where the Mg_2SiO_4 features appear.

The resulting Planck mean opacities are shown in Fig. 2. The solid line shows the absorption Planck mean per unit dust mass for the 195 M_{\odot} PISN model and the dashed line shows the same result for the 22 M_{\odot} model. When computing eq. (8), it is important to take into account the effect of dust sublimation: grains can be destroyed by heating

Table 1. Properties of dust grains produced in the ejecta of a $Z=0$, $22 M_{\odot}$ SNII and of a $195 M_{\odot}$ PISN. The table shows various grain species (first column), their mass fraction relative to the total dust mass produced (second and fourth columns), and their geometrical cross-sections (third and fifth columns). References for the adopted grain optical properties are given in the last column. In some cases, data was linearly extrapolated on the log-log plot to extend the original wavelength coverage to longer wavelengths.

Material	f_i	S_i	f_i	S_i	Optical properties
	$195 M_{\odot}$	$195 M_{\odot}$	$22 M_{\odot}$	$22 M_{\odot}$	
Al_2O_3	$5.82 \cdot 10^{-4}$	$4.82 \cdot 10^5$	$5.82 \cdot 10^{-3}$	$1.36 \cdot 10^6$	ISAS sample from Koike et al. (1995)
Fe_3O_4	$1.33 \cdot 10^{-2}$	$7.00 \cdot 10^4$	$2.88 \cdot 10^{-1}$	$2.58 \cdot 10^5$	Mukai (1989)
MgSiO_3	/	/	$5.24 \cdot 10^{-2}$	$3.22 \cdot 10^6$	Semenov et al. (2003)
Mg_2SiO_4	0.217	$6.30 \cdot 10^4$	$3.43 \cdot 10^{-1}$	$1.40 \cdot 10^6$	Semenov et al. (2003)
SiO_2	0.705	$5.58 \cdot 10^4$	/	/	Henning & Mutschke (1997); Philipp (1985)
AC (amorphous carbon)	$6.41 \cdot 10^{-2}$	$8.06 \cdot 10^4$	$3.11 \cdot 10^{-1}$	$8.50 \cdot 10^4$	ACAR from Zubko et al. (1996)

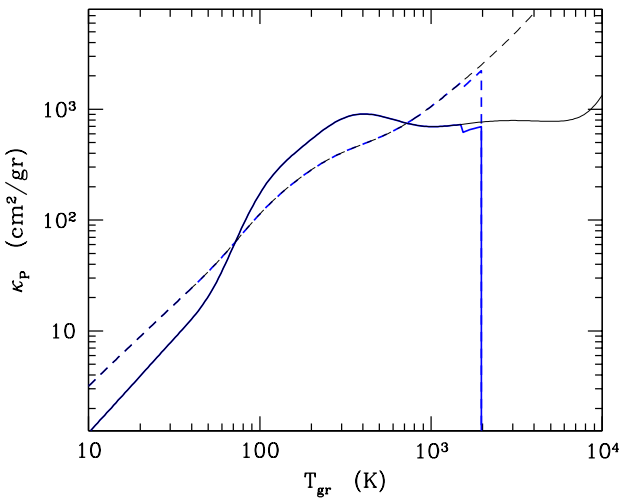


Figure 2. Planck mean opacities per unit dust mass for absorption for the $195 M_{\odot}$ PISN model (solid) and for the $22 M_{\odot}$ SN case (dashed). Thin lines assume that the grains never sublimate (see text).

through collisions with gas particles if the equilibrium grain temperature T_{gr} exceeds a characteristic value T_{sub}^i which, for each grain species i , depends on the gas density through the relative partial pressures of the heavy elements in the gas phase. Here we assume a sublimation temperature of $T_{\text{sub}}^{\text{AC}} = 2000$ K for AC grains and of 1500 K for other grain species (Laor & Draine 1993; Preibisch et al. 1993) and ignore the density dependence*. The thin lines in Fig. 2 show the results when sublimation is not considered.

2.2 H₂ formation on dust grains

An H atom can be bound to the grain surface in two energetically different sites: a physisorbed site, when the attractive forces are due to mutually induced dipole moments in the

* Note that comparable values are found for the condensation temperatures in the $195 M_{\odot}$ model, namely 2100 K for AC grains, 1800 K for Al_2O_3 , and 1470 K $< T < 1560$ K for the other grain species (see Todini & Ferrara 2001; Schneider et al. 2004).

electron shells of H and surface atoms (van der Waals interactions), and a chemisorbed site, when overlap between their respective wave-functions occur. Coming from the gas phase, the H atoms are first physisorbed and then either cross the barrier between the physisorbed and chemisorbed sites (by moving perpendicularly to the surface), or go to another physisorbed site (by moving along the surface). The relevant parameters which regulate grains surface characteristics are therefore the desorption energies of physisorbed H, E_{HP} , of chemisorbed H, E_{HC} , and of the saddle point between a physisorbed and a chemisorbed site, E_{S} , and can be derived by laboratory experiments for different grain species (see Cazeaux & Spaans 2004 and references therein)†.

At temperatures where the process of H₂ formation on grain surface is relevant in collapsing gas clouds, the most efficient reaction is the “collision” of two chemisorbed atoms, with efficiency (Cazeaux & Tielens 2002),

$$\epsilon_{\text{H}_2} = \left(1 + \frac{\beta_{\text{HP}}}{\alpha_{\text{PC}}}\right)^{-1} \quad (14)$$

where we have neglected the correction factor at high temperatures ($T > 300$ K) which reflects the evaporation of chemisorbed H. In the above equation, β_{HP} is the evaporation rate of physisorbed H and α_{PC} is the mobility to go from a physisorbed to a chemisorbed site, and their ratio can be approximated as (Cazeaux & Tielens 2002),

$$\frac{\beta_{\text{HP}}}{\alpha_{\text{PC}}} = \frac{1}{4} \left(1 + \sqrt{\frac{E_{\text{HC}} - E_{\text{S}}}{E_{\text{HP}} - E_{\text{S}}}}\right)^2 \exp\left[-\frac{E_{\text{S}}}{kT_{\text{gr}}}\right]. \quad (15)$$

The resulting H₂ formation rate per unit volume ($\text{cm}^{-3} \text{s}^{-1}$) on grain surface can be expressed as,

$$\begin{aligned} R_{\text{H}_2} &= \frac{1}{2} n(\text{H}) \bar{v}_{\text{H}} n_{\text{gr}} \sigma_{\text{gr}} \epsilon_{\text{H}_2} S_{\text{H}}(T) \\ &\equiv k_{\text{gr}} n(\text{H}) n_{\text{H}} \end{aligned} \quad (16)$$

where $n(\text{H})$ is the number density of H atoms in the gas phase, n_{H} is the number density of H nuclei (protons), and

† From Table 1 of Cazeaux & Spaans (2004), we take $E_{\text{HP}} = 800$ K, $E_{\text{HC}} = 3 \times 10^4$ K, and $E_{\text{S}} = 250$ K for AC grains. For other grain species we assume the same parameters as those derived for olivine (Mg_2SiO_4), namely $E_{\text{HP}} = 650$ K, $E_{\text{HC}} = 3 \times 10^4$ K, and $E_{\text{S}} = 200$ K

$S_{\text{H}}(T)$ is the sticking coefficient of H atoms which depends both on dust and gas temperatures (Hollenbach & McKee 1979),

$$S_{\text{H}}(T) = \left[1 + 0.4 \left(\frac{T+T_{\text{gr}}}{100 \text{ K}} \right)^{0.5} + 0.2 \left(\frac{T}{100 \text{ K}} \right) + 0.08 \left(\frac{T}{100 \text{ K}} \right)^2 \right]^{-1}. \quad (17)$$

Substituting eqs. (10) and (11) in eq. (16), the coefficient k_{gr} can be written as,

$$k_{\text{gr}} = \left(\frac{2kT}{m_{\text{H}}\pi} \right)^{1/2} S_{\text{H}}(T) \mathcal{D} m_{\text{H}} (1 + 4y_{\text{He}}) \Sigma_i f_i S_i \epsilon_{\text{H}_2}^i, \quad (18)$$

where $\epsilon_{\text{H}_2}^i$ is the H_2 recombination efficiency for each grain species.

3 RESULTS

3.1 Thermal evolution of collapsing clouds

Depending on the efficiency of metal diffusion and mixing, gas clouds in the vicinity of supernovae can be enriched to a wide range of metallicity values. If we assume that gas-phase metals and dust grains are not selectively transported, we can take the initial composition of pre-stellar gas clouds to reflect the final composition of SN ejecta. We then follow the thermal evolution of collapsing gas for a set of initial metallicities but relative metal and dust properties consistent with those predicted by the corresponding supernova model.

The results are shown in Fig. 3 for gas clouds with initial metallicities in the range $0 \leq Z/Z_{\odot} \leq 0.1$ enriched by the products of a $195 M_{\odot}$ PISN (left panel) and of a $22 M_{\odot}$ metal-free SNII (right panel). For these specific supernova models, dust depletion factors are predicted to be $f_{\text{dep}} = 0.65$ and 0.24 , respectively. Consistent with previous findings (Omukai 2000; Schneider et al. 2002, 2003; Omukai et al. 2005), at relatively low densities ($n_{\text{H}} \lesssim 10^5 \text{ cm}^{-3}$), thermal evolution is dominated by line-cooling of H_2 for $Z/Z_{\odot} \lesssim 10^{-5}$, of HD for $10^{-4} \lesssim Z/Z_{\odot} \lesssim 10^{-3}$, and, for $Z/Z_{\odot} \gtrsim 10^{-2}$, of O fine structure lines. Once the relevant cooling agent reaches the NLTE - LTE transition or the gas becomes optically thick to the dominant cooling radiation, line-cooling becomes inefficient and gravitational contraction leads to a temperature increase.

Note that, contrary to what commonly assumed, the above results suggest that C makes a negligible contribution to fine-structure line cooling, being strongly depleted onto AC grains and CO molecules for most SN models (Todini & Ferrara 2001; Schneider et al. 2004).

The impact of dust-cooling on the thermal evolution starts to be apparent for initial metallicities $Z/Z_{\odot} \gtrsim 10^{-6}$ ($Z \geq Z_{\text{cr}}$) as a temperature dip at high densities ($n_{\text{H}} \gtrsim 10^{13} \text{ cm}^{-3}$), which progressively shifts to lower densities for increasing total metallicity[†], until, for $Z/Z_{\odot} \gtrsim 10^{-2}$,

[†] If a larger amount of dust is present because the total metallicity of the gas is higher, then the corresponding cooling rate starts to be effective earlier in the evolution of collapsing gas clouds and it is not confined to the highest density regime.

the temperature dips due to line-cooling and dust-cooling merge and it is no-longer possible to separate the two contributions.

3.2 The impact of SN dust

It is interesting to compare the results of the self-consistent model for thermal evolution of collapsing clouds with previous studies, such as in Omukai et al. (2005), based on different assumptions on dust and metal properties. Comparing the tracks shown in Fig. 3 with the results in Fig. 1 of Omukai et al. (2005), we see that the temperature dip at high density ($n_{\text{H}} \sim 10^{13} \text{ cm}^{-3}$) due to dust-cooling which in the present analysis is already apparent in the $Z = 10^{-6} Z_{\odot}$ track, starts to be evident only at higher metallicities ($Z \geq 10^{-5} Z_{\odot}$) in Omukai et al. (2005). This result reflects a higher cooling efficiency of SN-dust with respect to present-day interstellar dust, partly due to larger grain cross-section and absorption coefficient per unit dust mass (eqs.12-13). Indeed, due the limited time available for grain-growth, SN-dust grains are smaller than present-day interstellar grains and the ratio of area to mass tends to be larger for smaller grains (Todini & Ferrara 2001; Nozawa et al. 2003; Schneider et al. 2004). A major difference is represented by the condensed C species adopted: in SN-dust models, C atoms condense in AC grains which are characterized by a high sublimation temperature (see section 2.1) and survive to the high-temperature environment of low-metallicity clouds. Conversely, following Pollack et al. (1994) all previous models assumed that C atoms condense in organics and therefore sublimate at lower temperatures, $\lesssim 600 \text{ K}$ (Omukai 2000; Schneider et al. 2003; Omukai et al. 2005).

The larger grain cross-section per unit mass of SN-dust enhances the H_2 formation rate. However, this has only a minor effect on the thermal evolutionary tracks at the lowest metallicities, being relevant only for $Z \gtrsim 10^{-4} Z_{\odot}$.

3.3 Fragmentation properties

Our main interest here is to investigate the fragmentation properties of clouds enriched by primordial supernovae, with the aim of understanding whether a preferred mass scale can be identified and eventually related to the characteristic mass of second-generation stars. Indeed, numerical simulations of primordial star formation have shown that in primordial environments, where magnetic fields, turbulence and rotation are likely to play a minor role in the dynamics, a preferred mass scale can be related to the Jeans mass at the end of the fragmentation process (see Bromm & Larson 2004 and references therein). More generally, Larson (2005) suggests that the low-mass, Salpeter-like IMF, which characterizes contemporary star formation, is determined largely by thermal physics and fragmentation in pre-stellar clouds.

Fragmentation occurs efficiently when the adiabatic index $\gamma = \text{dlog}p/\text{dlog}\rho < 1$, and almost stops when isothermality breaks ($\gamma > 1$) as also shown by the simulations of Li, Klessler & MacLow (2003). Thus, consistent with Schneider et al. (2002), (2003) we can adopt the condition $\gamma = 1$ to identify the preferred mass scale of the fragments (Inutsuka & Miyama 1997; Jappsen et al. 2005)

In Fig. 4 we plot the pre-stellar gas number density

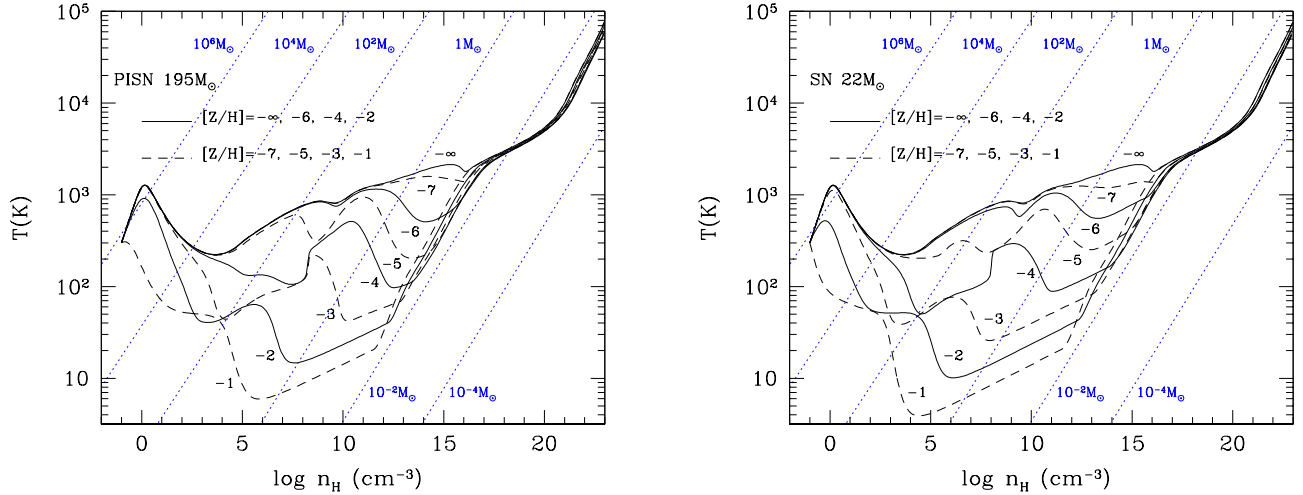


Figure 3. Thermal evolution of collapsing pre-stellar gas clouds as a function of the central gas number density enriched to different metallicities by the explosion of a PISN 195 M_{\odot} (left) and of a zero metallicity 22 SNII (right). Solid curves indicate total metallicities (gas-phase and solid dust grains) $[Z/H]=\text{Log}(Z/Z_{\odot}) = -\infty, -6, -4, -2$ and dashed curves to $[Z/H] = -7, -5, -3, -1$. The diagonal dotted curves identify values of the Jeans mass corresponding to given thermal states.

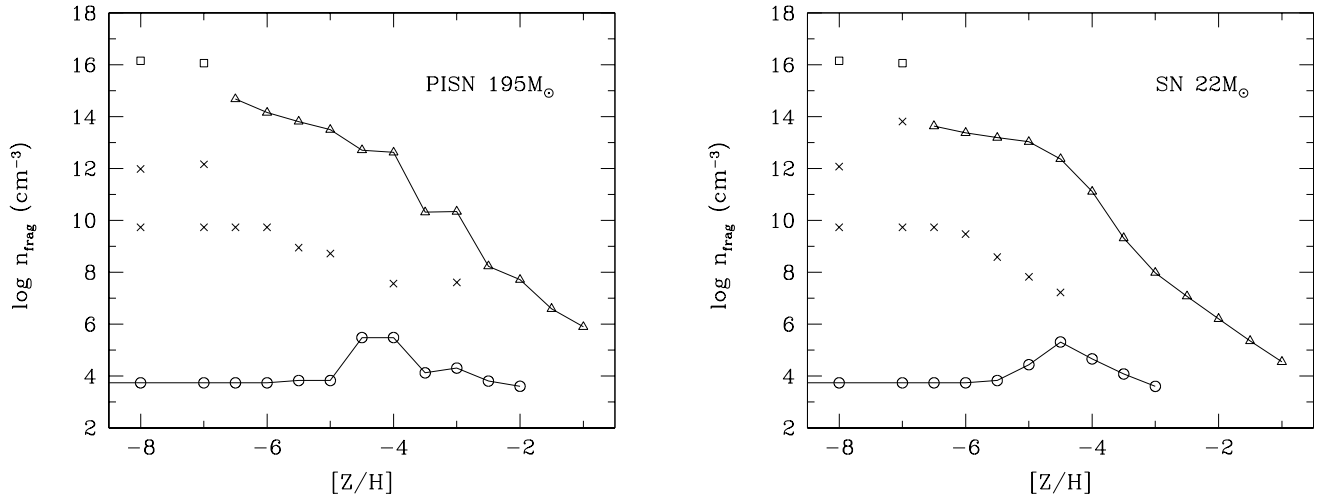


Figure 4. Gas number density where $\gamma = 1$ as a function of total metallicity (gas-phase γ metals and solid grains), for pre-stellar clouds enriched by the explosion of a 195 M_{\odot} PISN (left panel) and a 22 M_{\odot} SNII (right panel). Points indicated with circles (triangles) represent fragmentation induced by line (dust) cooling. Crosses show the effect of 3-body H_2 formation and H_2O cooling and, at the lowest metallicities, squares indicate fragmentation due to H_2 collision-induced emission (see text).

where this condition is met as a function of the initial total metallicity, for pre-stellar clouds enriched by the explosion of a 195 M_{\odot} PISN (left panel) and zero metallicity 22 M_{\odot} SNII (right panel). The “ $\gamma = 1$ ” points can be classified into three main branches: the lowest-density points, shown as open circles, indicate fragmentation epochs which follow the temperature dip induced by line-cooling (hereafter line-induced fragmentation); the highest-density points represent fragmentation following cooling due to H_2 collision-induced emission at the lowermost metallicities (squares) and due to dust thermal emission (hereafter dust-induced fragmentation) at higher metallicities (triangles); for completeness, we also show a third branch of $\gamma = 1$ points (crosses) which corresponds to gas number densities $n_{\text{frag}} \sim 10^{10} \text{ cm}^{-3}$, and which is associated to cooling by 3-body H_2 formation and

H_2O . As it can be inferred from Fig. 3, the cooling rate at these intermediate densities leads to temperature decrements which tend to be short-lived and shallow and are unlikely to induce fragmentation. The local maxima of the line-induced fragmentation branch result from the competition between HD cooling (which starts to be effective at $Z \gtrsim 10^{-5} Z_{\odot}$) and heating due to H_2 formation on grain surface which, for $Z \gtrsim 10^{-4} Z_{\odot}$ prevents the gas from reaching the NLTE-LTE transition for HD at densities $n \sim 10^5 \text{ cm}^{-3}$.

It is important to stress that the presence of a temperature dip in the thermal evolutionary track as well as the condition that $\gamma < 1$ imply only the possibility of fragmentation. For clouds of solar metallicity, recent three-dimensional hydrodynamical simulations show that the single temperature minimum present at a density comparable to that of

observed cloud cores plays an important role in determining the peak mass of the IMF (Jappsen et al. 2005). In contrast, the second minimum in the thermal evolutionary track due to dust-cooling occurs at a density which is several order of magnitudes higher, deep in the interior of the collapsing cloud. Therefore, it is not clear whether the same argument may be applied as well as the fraction of mass which may be affected.

Dust-induced fragmentation will occur if very flattened or elongated structures form in the dense central region, and if the fragments formed do not subsequently merge. Indeed, following the first line-induced fragmentation, pre-stellar gas clouds experience runaway collapse, during which density perturbations might be erased by pressure forces. If so, with little elongation of the densest core, dust-induced fragmentation at higher densities would be prohibited. By means of a semi-analytic model for the linear evolution of non-spherical deformations, Omukai et al. (2005) discuss the fragmentation histories of collapsing pre-stellar clouds and confirm that dust-induced fragmentation does occur even for metallicities as low as $Z = 10^{-6}Z_{\odot}$. The mass fraction in low-mass fragments is initially small but becomes dominant for $Z \gtrsim 10^{-5}Z_{\odot}$ and continues to grow with increasing Z . More recently, Tsuribe & Omukai (2006) used three-dimensional hydrodynamical simulations to follow the evolution of low-metallicity cores during the dust-cooling phase and discuss the conditions for fragmentation into low-mass clumps. Their results confirm that the previous analysis of Omukai et al. (2005) was broadly correct: fragmentation does occur in the dust-cooling phase and sub-solar mass fragments are indeed produced.

3.4 Characteristic mass

In the present context, where we assume that thermal pressure is the main force opposing gravity, the characteristic mass of each fragment is given by the Jeans mass at fragmentation epoch,

$$M_{\text{frag}} = M_J(n_{\text{frag}}, T_{\text{frag}}) \propto \rho \lambda_J^3 \propto T_{\text{frag}}^{3/2} n_{\text{frag}}^{-1/2}.$$

Fig. 5 shows the Jeans masses associated to the lower and upper density branches represented in Fig. 4, hence to line-induced and dust-induced fragmentation. Since line-induced fragmentation occurs at relatively low densities, the corresponding fragment masses are large. In particular, at the lowest metallicities we find that the characteristic fragmentation mass scale, induced by H_2 line cooling, is $M_{\text{frag}} \sim 10^3 M_{\odot}$, consistent with the results of numerical models. Still, even for total metallicities in the range $10^{-5} \leq Z/Z_{\odot} \leq 10^{-2}$, metal-line cooling leads to fragment masses $M_{\text{frag}} \geq 100 M_{\odot}$.

Conversely, dust-induced fragmentation leads to solar or sub-solar mass fragments, with $0.01 M_{\odot} \leq M_{\text{frag}} \leq 1 M_{\odot}$. Indeed, this fragmentation mode occurs at much higher densities (see Fig. 4) where the associated Jeans masses are correspondingly lower. The characteristic fragment mass increases for increasing metallicity reflecting the opposite trend in the dust-induced fragmentation density shown in Fig. 4. For both supernova models, this fragmentation mode is active already at very low metallicities and the solid line illustrates the transition in fragmentation mass scales for $Z_{\text{cr}} = 10^{-6}Z_{\odot}$.

The importance of dust for the formation of low-mass stars was first emphasized by the pioneering work of Low & Lynden-Bell (1976), where they also recognized that dust maintains its cooling efficiency down to a reduction by mass of 10^{-5} of the present-day value.

The results that we find suggest that in the absence of dust pre-stellar clouds enriched by primordial supernovae are not able to form solar or sub-solar mass fragments.

4 DISCUSSION

In this paper we have presented the first self-consistent model of thermal evolution of pre-stellar gas clouds enriched with metals and dust by primordial supernovae. We have focused on two representative cases: a $195 M_{\odot}$ pair-instability supernova and a $22 M_{\odot}$ TypeII supernova. Using the one-zone semi-analytic model initially developed by Omukai (2000), and recently improved in Omukai et al. (2005), we have followed the thermal and fragmentation history of pre-stellar clouds enriched by the products of single primordial supernovae. We have sampled initial metallicities in the range $0 \leq Z/Z_{\odot} \leq 0.1$, as representative of different enrichment histories, which may vary depending on metal diffusion and mixing.

Neglecting differential enrichment by metals and dust grains, the initial composition of the collapsing pre-stellar gas clouds directly reflects the nucleosynthetic products of the polluting SN, its specific dust depletion factor, relative gas-phase metal abundances and dust grain species and sizes. We have therefore modified the model to allow a self-consistent description of metal-line cooling, dust thermal emission, dust-gas collision rate, H_2 formation rate on dust grains. In all theoretical studies carried out so far, these processes were implemented under the implicit assumption that the gas-phase metal abundances and dust grain properties were the same as those observed in the local interstellar medium. The only exception is the study of Bromm & Loeb (2003), where separate critical abundances of CII and OI enabling cooling and fragmentation in collapsing gas clouds were derived. Still, they limited their study to the thermal evolution in the low-density regime, including only metal line cooling and fragmentation.

The main results of our study can be summarized as follows:

- (i) As long as thermal physics is considered to play a major role in setting a characteristic stellar mass scale, dust-induced fragmentation appears to be the most promising mechanism for the formation of solar and sub-solar mass fragments. Since dust can be promptly synthesized in the ejecta of primordial SN, it is likely that its contribution to thermal and fragmentation history of collapsing clouds at high redshifts had been relevant.
- (ii) Due to the strong depletion of C atoms onto AC grains and CO molecules for most SN models, our analysis shows that CII makes a negligible contribution to fine-structure line cooling, leaving OI as the main cooling agent in the gas phase.
- (iii) Line-cooling, being limited to the initial evolution of collapsing gas clouds, for densities in the range $10^4 - 10^6 \text{ cm}^{-3}$, induces fragmentation into relatively

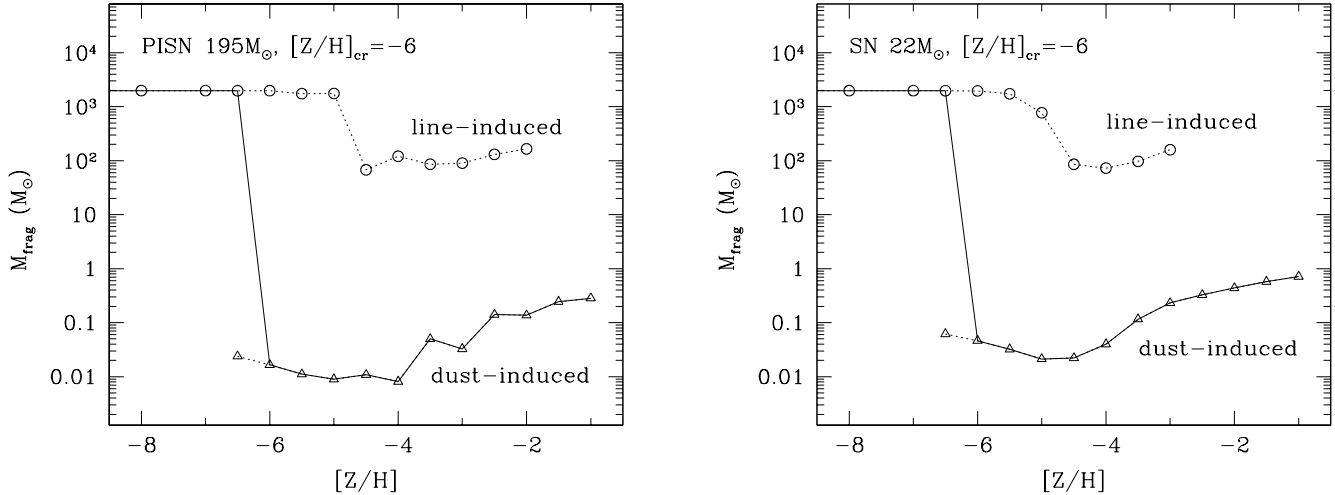


Figure 5. Thermal Jeans mass corresponding to line-induced fragmentation (circles in Fig. 4) and dust-induced fragmentation (triangles in Fig. 4) as a function of total metallicity, for pre-stellar clouds enriched by the explosion of a 195 M_{\odot} PISN (left panel) and a 22 M_{\odot} SNII (right panel). The solid line indicates the transition in characteristic fragment masses when the dust-induced fragmentation mode is activated at a critical metallicity $Z_{\text{cr}} = 10^{-6} Z_{\odot}$.

large clumps, with characteristic fragment masses $M_{\text{frag}} \geq 100 M_{\odot}$, even for initial gas metallicities $Z \lesssim 10^{-2} Z_{\odot}$.

(iv) The formation of solar or sub-solar mass fragments might operate already at metallicities $Z_{\text{cr}} = 10^{-6} Z_{\odot}$. The results that we find suggest a re-formulation of the critical metallicity scenario: indeed, once a self-consistent model is adopted, the presence of gas-phase metals can not by itself lead to solar or sub-solar characteristic masses whereas primordial supernovae of all masses (that is both in the standard SNII mass range and in massive PISN), appear to deplete enough metals in solid grains to enable the formation of low-mass fragments.

Our approach to determine the minimum fragment masses as the Jeans masses corresponding to the last fragmentation (temperature dip and $\gamma = 1$ condition) may be an oversimplification of the complex dynamical evolution of cloud cores. Still, our findings are supported by results of a semi-analytical model for the linear evolution of non-spherical deformations by Omukai et al. (2005) and by three-dimensional hydrodynamical simulations of Tsuribe & Omukai (2006), which confirm that fragmentation occurs during the dust-cooling phase and that sub-solar mass fragments are indeed produced.

Let us emphasize that other processes might be equally important in reducing the characteristic mass scales of metal-free or very metal-poor star forming regions. Among these, the bimodal IMF suggested by Umemura & Nakamura (2002), the presence of a strong UV field in the vicinity of a very massive star (Omukai & Yoshii 2003), HD cooling triggered in relic HII regions around very massive stars after the death of the exciting star (Uehara & Inutsuka 2000; Nagakura & Omukai 2005; Johnson & Bromm 2006), shock-compression induced by the first SN explosions (MacKey, Bromm & Hernquist 2003; Salvaterra, Ferrara & Schneider 2004).

Observationally, stellar relics in the halo of our Galaxy represent fundamental records of low-mass star formation at high redshifts. The HK-survey, Hamburg-ESO Prism Sur-

vey and Sloan Digital Sky Survey provide already a sample of about 5000 stars with $[\text{Fe}/\text{H}] < -2$, among which 750 with $[\text{Fe}/\text{H}] < -3$. The project SEGUE (Sloan Extension for Galaxy Understanding and Exploration) should identify about 25000 stars with $[\text{Fe}/\text{H}] < -2$ (Beers & Christlieb 2005). The interpretation of shape and low-metallicity tail of the metallicity distribution function should provide important insights on the origin of the first low-mass stars that have formed in the Universe (Schneider et al. 2003; Tumlinson 2006; Salvadori, Schneider & Ferrara 2006).

The surface elemental abundances of the observed stellar relics should shed light on the IMF of the stars mostly responsible for early metal enrichment (Tumlinson, Venkatesan & Shull 2004; Iwamoto et al. 2005; Beers & Christlieb 2005). In principle, dust depletion does not affect the interpretation of the observed chemical abundances because, once sufficiently high central densities are reached, dust grains present in collapsing pre-stellar clouds are destroyed and the original gas-phase metal abundances (reflecting the nucleosynthetic products of the SN progenitor star) are re-established. An alternative scenario has been recently proposed by Venkatesan, Nath & Shull (2006), who suggest that the elements forming the composition of the dominant dust compounds created in primordial supernovae (Si, Mg, O, C) can be selectively transported in the UV radiation field from the first stars and decoupled from the background SN metals in the gas phase. Interestingly, these elements appear to have enhanced abundances in the most metal poor halo stars observed.

ACKNOWLEDGMENTS

We thank S.Bianchi, H. Hirashita & T.Kozasa for providing some of the data on grain optical properties in a machine readable form and S.Bianchi for useful comments on the manuscript.

REFERENCES

- Abel, T., Brian, G. & Norman, M. L. 2002, *Science*, 295, 93
- Bertoldi, F. et al. 2003, *A&A*, 406, L55
- Bromm, V., Ferrara, A., Coppi, P. & Larson, R. B. 1999, *MNRAS*, 328, 969
- Bromm, V., Coppi, P. & Larson, R. B. 2002, *ApJ*, 564, 23
- Bromm, V. & Loeb, A. 2004, *New Astronomy*, 9, 353
- Bromm, V. & Larson, R. B. 2004, *ARA&A*, 42, 79
- Cazaux, S. & Tielens, A. 2002, *ApJ*, 575, L29
- Cazaux, S. & Spaans, M. 2004, *ApJ*, 611, 40
- Beers, T. C., Christlieb, N. 2005, *ARA&A*, 43, 531
- Galli, D. & Palla, F. 1998, *A&A*, 335, 403
- Green, D. A., Tuffs, R. J., Popescu, C. C. 2004, *MNRAS*, 355, 1315
- Henning, T. & Mutscke, H. 1997, *A&A*, 327, 743
- Hines, D. C. 2004, *APJS*, 154, 290
- Hollenbach, D., McKee, C. F. 1979, *ApJS*, 41, 555
- Inutsuka, S. & Miyama, S. M. 1997, *ApJ*, 480, 681
- Iwamoto, N., Umeda, H., Tominaga, N., Nomoto, K., Maeda, K. 2005, *Science*, 309, 451
- Jappsen, A. K., Klessen R. S., Larson, R. B., Li, Y. & Mac Low, M. M. 2005, *A&A*, 435, 611
- Johnson, J. L. & Bromm, V. 2006, *MNRAS*, 366, 247
- Koike, C., Kaito, C., Yamamoto, T., Shibai, H., Kimura, S., Suto, H. 1995, *Icarus*, 114, 203
- Kozasa, T., Hasegawa, H. & Nomoto, K. 1989, *ApJ*, 344, 325
- Krause, O. et al. 2004, *Nature*, 432, 596
- Laor, A. & Draine, B. T. 1993, *ApJ*, 402, 441
- Larson, R. B. 2005, *MNRAS*, 359, 211
- Li, Y., Klessen, R. S. & Mac Low, M. M. 2003, *ApJ*, 592, 975
- Low, C. & Lynden-Bell, D. 1976, *MNRAS*, 176, 367
- MacKey, J., Bromm, V. & Hernquist, L. 2003, *ApJ*, 586, 1
- Maiolino, R., Schneider, R., Oliva, E., Bianchi, S., Ferrara, A., Mannucci, F., Pedani, M., Roca Sogorb, M. 2004, *Nature*, 431, 533
- Morgan, H. L. & Edmunds, M. G. 2003, *MNRAS*, 343, 427
- Morgan, H. L., Dunne, L., Eales, S. A., Ivison, R. J., Edmunds, M. G. 2003, *ApJ*, 597, L33
- Nagakura, T. & Omukai, K. 2005, *MNRAS*, 364, 1378
- Nakamura, F. & Umemura, M. 2002, *ApJ*, 569, 549
- Mukai, T. 1989, in *Evolution of interstellar dust and related topics*, Proceedings of the International School of Physics “Enrico Fermi” eds A. Bonetti, J.M. Greenberg, S. Aiello, Elsevier Science Publisher, New York, pg. 397
- Nozawa, T., Kozasa, T., Umeda, H., Maeda, K., & Nomoto, K. 2003, *ApJ*, 598, 785
- Omukai, K. & Nishi, R. 1998, *ApJ*, 508, 141
- Omukai, K. 2000, *ApJ*, 534, 809
- Omukai, K. & Palla, F. 2003, *ApJ*, 589, 677
- Omukai, K. & Yoshii, Y. 2003, *ApJ*, 599, 746
- Omukai, K., Tsuribe, T., Schneider, R., Ferrara, A. 2005, *ApJ*, 626, 627
- Philipp, 1985, in *Handbook of optical constants of solids*, ed E. D. Palik, Academic Press, New York, pg. 719
- Pollack, J. B., Hollenbach, D., Beckwith, S., Simonelli, D. P., Roush, T., Fong, W. 1994, *ApJ*, 421, 615
- Preibisch, Th. Ossenkopf, V. Yorke, H. W. Henning, Th. 1993, *A&A*, 279, 577
- Priddey, R. S., Isaak, K. G., McMahon, R. G., Robson, E. I., Pearson, C. P. 2003, *MNRAS*, 344, L74
- Salvaterra, R., Ferrara, A., Schneider, R. 2004, *New Astronomy*, 10, 113
- Schneider, R., Ferrara A., Natarajan P., Omukai K. 2002, *ApJ*, 571, 30
- Schneider, R., Ferrara A., Salvaterra R., Omukai K., Bromm V. 2003, *Nature*, 422, 869
- Schneider, R., Ferrara, A. & Salvaterra, R. 2004, *MNRAS*, 351, 1379
- Salvadori, S., Schneider, R., Ferrara, A. 2006, in preparation
- Semenov, D., Henning, T., Helling, C., Ilgner, M., Sedlmayr, E. 2003, *A&A*, 410, 611
- Tan, J., McKee, C. F. 2004, *ApJ*, 603, 383
- Todini, P. & Ferrara, A. 2001, *MNRAS*, 325, 726
- Tsuribe, T. & Omukai, K. 2006, *ApJL*, in press
- Tumlinson, J., Venkatesan, A., Shull, J. M. 2004, *ApJ*, 612, 602
- Tumlinson, J. 2006, submitted to *ApJ*, pre-print astro-ph/0507442
- Uehara, H. & Inutsuka, S. 2000, *ApJ*, 531, L91
- Venkatesan, A., Nath, B. B. & Shull, J. M. 2006, to appear in *ApJ*, 640, 20 March 2006 issue pre-print astro-ph/0508163
- Wilson, T. L., Batrla, W. 2005, *A&A*, 430, 561
- Zubko, V. G., Mennella, V., Colangeli, L., Bussoletti, E. 1996, *MNRAS*, 282, 1321